$A\beta_{1-42}$ stimulates actin polymerization in hippocampal neurons through Rac1 and Cdc42 Rho GTPases

Ariadna Mendoza-Naranjo[1,*], Christian Gonzalez-Billault[1] and Ricardo B. Maccioni[1,2]

[1]Laboratory of Cellular, Molecular Biology and Neuroscience, Department of Biology, Faculty of Sciences and [2]Department of Neurological Sciences, Universidad de Chile, Las Palmeras 3425, Nunoa, Santiago, Chile

*Author for correspondence (e-mail: amendoza@med.uchile.cl)

Accepted 30 October 2006
Journal of Cell Science 120, 279-288 Published by The Company of Biologists 2007
doi:10.1242/jcs.03323

Summary

A number of psychiatric and neurodegenerative disorders, such as Alzheimer's disease, are characterized by abnormalities in the neuronal cytoskeleton. Here, we find that the enhancement in actin polymerization induced by fibrillar amyloid-beta peptide (Aβ) is associated with increased activity of Rac1/Cdc42 Rho GTPases. Rac1 upregulation involves the participation of Tiam1, a Rac guanine-nucleotide exchange factor, where Aβ exposure leads to Tiam1 activation by a Ca^{2+}-dependent mechanism. These results point to Rho GTPases as one of the targets in Aβ-induced neurodegeneration in Alzheimer's disease pathology, with a role in mediating changes in the actin cytoskeletal dynamics.

Supplementary material available online at
http://jcs.biologists.org/cgi/content/full/120/2/279/DC1

Key words: Alzheimer's disease, Amyloid beta, Rac1 Cdc42 Rho GTPases, Actin polymerization, Tiam1

Introduction

Abnormalities in cytoskeletal organization are a common feature of many neurodegenerative disorders, including Alzheimer's disease (AD). Pathological actin in a polymerized conformation (F-actin) has been found throughout Hirano bodies (Galloway et al., 1987; Goldman, 1983), which are cytoplasmic inclusions found in several neurodegenerative diseases, including AD (Gibson and Tomlinson, 1977). Actin is also a component of cofilin-actin rods [inclusion-like structures described in hippocampal and cortical neurons of post-mortem AD brains and also induced by certain chemical or physical stresses in cultured cells (Minamide et al., 2000)], which are thought to be associated with neurodegeneration.

The Rho family of small GTPases (Rho, Rac and Cdc42) are regulators of F-actin polymerization (Bishop and Hall, 2000), acting as molecular switches by cycling between an inactive GDP-bound state and an active GTP-bound state. Rac1 and Cdc42 promote polymerization at the leading edge, orchestrating the formation of lamellipodia and membrane ruffles (Ridley et al., 1992), as well as peripheral actin microspikes and filopodia (Kozma et al., 1995; Nobes and Hall, 1995). RhoA is an antagonist, promoting retraction of the leading edge and assembly of stress fibers (Schmitz et al., 2000).

Rho GTPase activation at the plasma membrane depends on the geranylgeranyl lipid residue attached to the C terminus of the GTPase proteins (Seabra, 1998) and requires the interaction with guanine nucleotide exchange factors (GEF) that can stimulate the exchange of GDP for GTP, allowing the Rho-family GTPases to bind to and activate their effector proteins. Tiam1 is a protein that functions as a GEF for Rac1 GTPase, both in vitro and in vivo (Habets et al., 1994). Tiam1 requires phosphorylation at threonine residues by calcium/calmodulin kinase II (CaMK-II) and protein kinase C (PKC) that may elicit the activation and/or translocation of the protein to the membrane compartment (Fleming et al., 1999; Fleming et al., 1997). Tiam1 translocation to the plasma membrane induces membrane ruffles and JNK stimulation mediated by Rac1, suggesting that the control of membrane association of Tiam1 is an important factor in Rac1 activation (Michiels et al., 1997).

Deregulation of the Rho GTPase pathway is implicated in several pathological conditions, including neurodegenerative disorders like AD. This pathology is characterized by a progressive loss in the number of dendritic spines, as well as by alterations in the synaptic efficacy and damage at the synaptic terminal (Lippa et al., 1992; Masliah, 1995). The dynamic regulation of actin polymerization is considered the main mechanism underlying morphological changes in dendritic spines (Matus, 2000; Halpain, 2000). Rac1/Cdc42 Rho GTPases, which are the main regulators of F-actin polymerization, have been implicated in the maintenance and reorganization of dendritic structures (Nakayama et al., 2000; Luo, 2000). Neuronal populations of AD patients showed a considerable overlap of Rac/Cdc42 with early cytoskeletal abnormalities, as well as Rac/Cdc42 upregulation in cases of AD in comparison with an age-matched control (Zhu et al., 2000). We found an increase in Rac1 immunoreactivity in cortex sections derived from Tg2576 (Otth et al., 2003), a transgenic mouse model expressing the Swedish mutation of the human amyloid precursor protein that causes memory deficits and plaque accumulation with age (Hsiao et al., 1996). Rac1 is also an essential element of the amyloid-beta signaling cascade that leads to the generation of ROS in astroglioma cells (Lee et al., 2002).

In neurons, amyloid-beta (Aβ) peptide (the main constituent of the neuritic plaque) destabilizes Ca^{2+} regulation and renders neurons more vulnerable to environmental stimuli that elevate

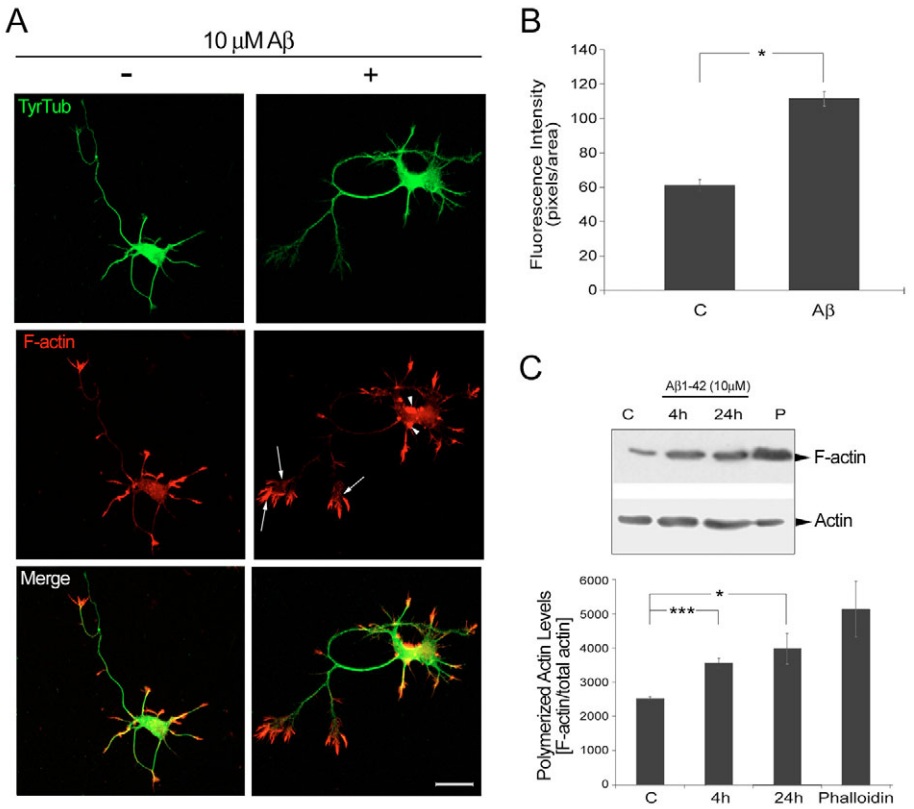

Fig. 1. F-actin levels are increased in hippocampal neurons treated with Aβ. (A) Control hippocampal neurons grown on poly-D-lysine for 4 days were stimulated with 10 μM of fibrillar $A\beta_{1\text{-}42}$ for 4 hours and double stained for Tub-Tyr (green) and F-actin filaments with Rhodamine-phalloidin. Overlay of Tub-Tyr with phalloidin is shown. Scale bar, 20 μm. (B) Hippocampal cells, untreated or stimulated for 4 hours with 10 μM $A\beta_{1\text{-}42}$ were immunostained with phalloidin-TRITC and the F-actin intensity was analyzed. The values are expressed as the main ± s.e.m. Data are representative for three different experiments, with at least 12 determinations per experiment (*P<0.05). (C) F-actin levels in control and 4-hour and 24-hour Aβ-stimulated neurons were measured with Actin Polymerization Assay kit. Phalloidin (P) was used as a positive control. The ratio of F-actin/total actin was determined from the blots by densitometric measurements. Significant differences are indicated by asterisks (*P<0.05, ***P<0.005; Student's t-test).

intracellular Ca^{2+} levels (Mattson et al., 1993). Correspondingly, it has also been seen that an increase in intracellular Ca^{2+} induces membrane translocation and activation of Rac, an event dependent on the activation of conventional protein kinase C (PKC) (Price et al., 2003). In Swiss 3T3 fibroblasts, the Ca^{2+} chelator BAPTA-AM totally abrogated Tiam1 phosphorylation induced by PDGF, indicating that Ca^{2+} is essential for Tiam1 activation (Fleming et al., 1998). These results suggest that Ca^{2+} is an essential regulator of Rac/Tiam1signaling.

We have studied alterations in the actin cytoskeleton in Aβ-stimulated neurons and the involvement of Rac/Cdc42 Rho GTPases and associated regulators in these changes.

Results

Aβ peptide increases F-actin in hippocampal cells

The presence of structures characterized by aggregates of polymerized actin (F-actin) has been described in AD. In order to test whether Aβ presence could be related with the formation of this kind of structures, we cultured hippocampal cells in the presence of 10 μM $A\beta_{1\text{-}42}$, an accepted neurodegeneration model for AD. Such Aβ concentrations have been detected in brain tissues of AD patients and mice transfected with human amyloid precursor protein gene (Kuo et al., 1999; McLean et al., 1999; Kawarabayashi et al., 2001; Funato et al., 1998), and are pathophysiologically relevant. The F-actin content was examined by Rhodamine-phalloidin staining. An antibody that recognizes tyrosinated tubulin (TyrTub) was also added, as a dynamic microtubules marker. After short periods of fibrillar peptide exposure (30 minutes to 2 hours) no visual changes in actin polymerization were detected in neurons stained with Rhodamine-phalloidin (data not show). Four hours after Aβ stimulation, a noticeable increase of F-actin was observed in comparison to control neurons (Fig. 1A), without changes in the TyrTub stain. This increase in polymerized actin was reflected by an augmentation in the formation of membrane ruffles (Fig. 1A, arrowheads), as well as in filopodia and lamellipodia, in minor processes and in the distal tip of the growing axon (Fig. 1A, arrows). In order to quantify the observed increase, we measured the F-actin content in control and Aβ-treated hippocampal neurons immunostained with Rhodamine-phalloidin. This analysis revealed a statistically significant increase of over 60% in the amount of F-actin after Aβ treatment (Fig. 1B).

We also measured changes in the F-actin content after $A\beta_{1\text{-}42}$ stimulation, using an In Vivo Actin Dynamic Assay kit. Four hours after the treatment with Aβ, the same time at which a significant increase in actin polymerization was observed (Fig. 1A), a 40% rise in F-actin content was detected, and maintained after 24 hours of Aβ-treatment (Fig. 1C). In addition, the cell homogenate was incubated with phalloidin, as a positive control for F-actin formation, displaying higher amounts of F-actin than control and Aβ-treated cells (Fig. 1C, lane P). To further analyze these changes in actin cytoskeleton, morphometric parameters, such as filopodia number and growth cone area, were measured. Fig. 2 shows that the enhancement in F-actin polymerization after Aβ treatments was accompanied by a significant increase in the size of the growth cone area (P<0.05), as well as in the number of filopodia (P<0.001), when compared with controls.

Activation of Rac1 and Cdc42 is responsible for increased F-actin in Aβ-treated cells

Rho GTPases are key regulators of F-actin polymerization. In

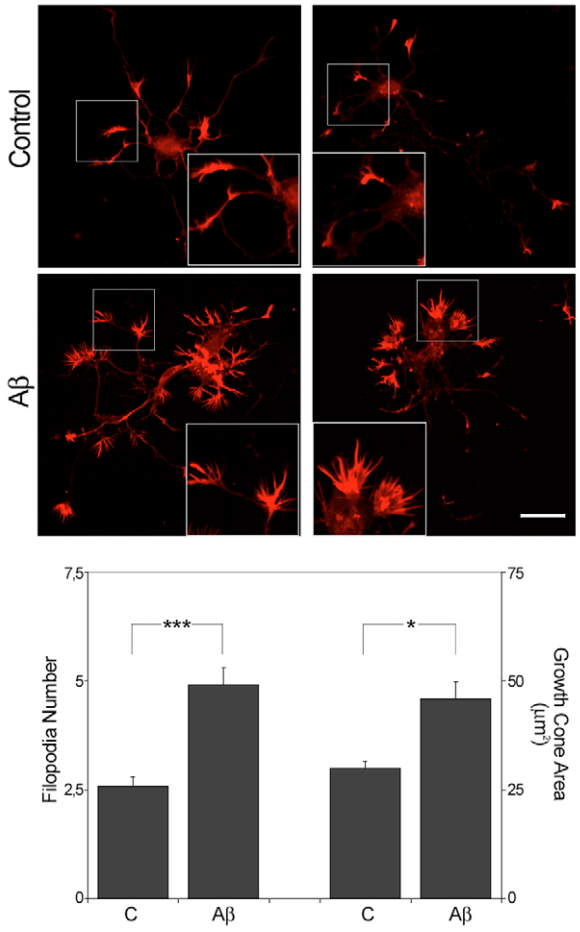

Fig. 2. Increase in F-actin levels correlates with enhancement in growth cone area and filopodia number. Hippocampal neurons control and stimulated with $A\beta_{1\text{-}42}$ were immunostained with phalloidin-TRITC (top panels; higher magnification of the boxed regions is shown in the insets) and growth cone area and filopodia number were analyzed (bottom panels). Scale bar, 20 μm. Values are expressed as mean ± s.d.

order to analyze whether F-actin increased polymerization by Aβ is dependent of Rac1/Cdc42 activation, PBD [p21-activated kinase-(PAK)-binding domain] was used. The amount of activated Rac1/Cdc42 was determined after treatment with different doses of the amyloid peptide. Activation of Rac was dose dependent, so that 10 μM $A\beta_{1\text{-}42}$, the highest concentration tested, rendered the greatest Rac/Cdc42-GTP levels (Fig. 3A; see also supplementary material Fig. S1). Quantitative analysis indicated that the active pool of Rac1 increased 1.6-fold after the addition of Aβ in comparison to the untreated condition (Fig. 3A). This effect was time-dependent with significant differences found between the control and 4 hours, as well as between the control and 24 hours of peptide incubation (Fig. 3B). In parallel, $A\beta_{1\text{-}42}$ increased the activation of Cdc42 also in a time- and dose-dependent manner (see supplementary material Fig. S1).

To verify the specificity of the activation of Rac1 and Cdc42 GTPases in the signaling pathway mediated by the amyloid peptide, the addition of $A\beta_{1\text{-}42}$ was combined with pertussis toxin (PTX), a G-protein inhibitor affecting Rac1 and Cdc42 activation (Van Leeuwen et al., 2003). PTX partially inhibited the increases in Rac1 and Cdc42 after Aβ addition (Fig. 3C,D). Cyclin-dependent kinase 5 (Cdk5), which is deregulated in Alzheimer brains (Alvarez et al., 1999; Patrick et al., 1999) and probably contributes to the pathogenesis of the disease, colocalizes with Rac1 in neuronal growth cones (Nikolic et al., 1998). Hippocampal cells treated with $A\beta_{1\text{-}42}$ along with roscovitine, a Cdk5 inhibitor, exhibited the same extent of Rac1 activation as those stimulated without the inhibitor (Fig. 3C).

To further investigate the role of Rac1 and Cdc42 in Aβ induction of actin polymerization, changes in the distribution of both proteins and their relationship with F-actin after stimulation with the peptide were examined. Aβ treatments induced actin remodeling and increased the amount of actin-dependent structures (Fig. 4A, arrows), accompanied by enhanced colocalization of Rac1 and Cdc42 with F-actin-rich domains (Fig. 4A, arrowheads). The extent of Aβ-induced Rac1-F-actin and Cdc42-F-actin colocalization was evaluated in two-dimensional scatter analyses of fluorescence intensity distribution. Fig. 4B shows that Aβ stimulation promoted an increase in the colocalization of Rac1 and Cdc42 with polymerized actin. In order to confirm this increase, we determined the colocalization coefficient obtained from the merged images that display the intensity and distribution of red and green pixels. Amyloid-treated neurons stained for Rac1 and phalloidin displayed higher colocalization coefficients than those showed for control untreated neurons (Fig. 4C). Similar results were obtained for Cdc42 and phalloidin-labeled samples.

Translocation of Rac1 and Cdc42 to the cell plasma membrane is essential for activating downstream effectors. To determine whether Rac1 and Cdc42 are recruited to the cell membrane after Aβ stimulation, hippocampal cultures were fixed after detergent extraction, which was performed under microtubule-stabilizing conditions. This method removes soluble proteins from the cell in a way that proteins remaining are attributable to the polymerized fraction (Brown et al., 1992). Samples were processed for immunofluorescence in cells fixed after detergent extraction, by double immunostaining with Rac1 or Cdc42 antibodies, along with Rhodamine-phalloidin. Rac1 and Cdc42 were mostly localized in the neuronal body and throughout the processes, and were preferentially recruited to the cell membrane after Aβ stimulation (Fig. 5A, green stain), where they were frequently found colocalizing with Rhodamine-phalloidin (Fig. 5A, arrowheads).

In order to verify the results from the immunofluorescence experiments, Rac1 and Cdc42 association with the membrane fraction was analyzed, using subcellular fractionation protocols. When hippocampal neurons were stimulated with 10 μM fibrillar $A\beta_{1\text{-}42}$ an increase in the translocation of both proteins from the cytosolic to the membrane fraction was observed, characterized by the presence of flotillin (Fig. 5B), reinforcing the results of GTPases activation by amyloid treatments. Membrane fractions were negative for NFκB, confirming that these fractions were devoid of cytoplasmic contamination (data not shown).

Rac1 and Cdc42 activity can be changed by mutations leading to either constitutively active or dominant-negative forms. To further demonstrate the involvement of these proteins

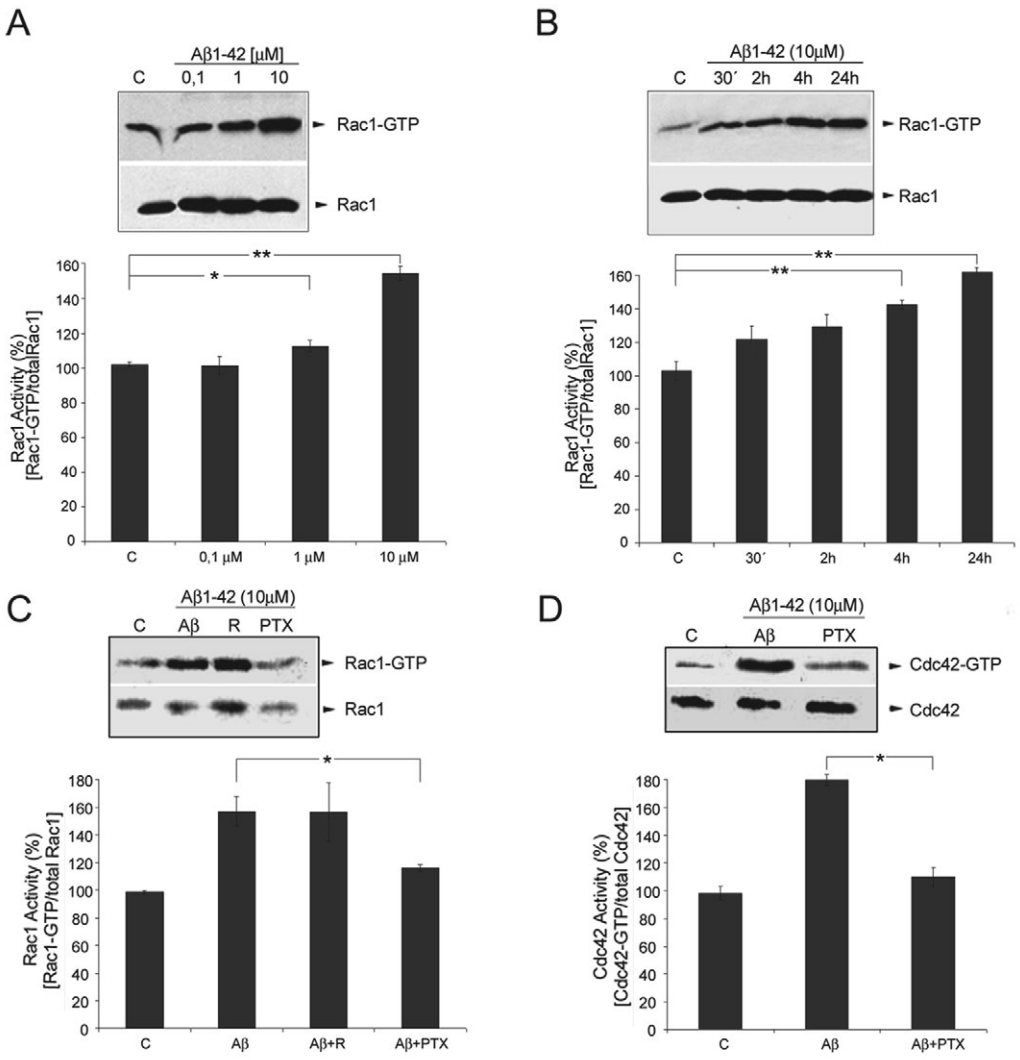

Fig. 3. GTPase activities of Rac1 and Cdc42-GTPase are increased in neurons stimulated with $A\beta_{1\text{-}42}$. Hippocampal neurons cultured for 4 days were treated with (A) 0.1, 1 and 10 μM $A\beta_{1\text{-}42}$ for 24 hours and (B) with 10 μM of peptide for 30 min, 2, 4 and 24 hours. Active GTP-Rac1 was pulled down using the PAK-PBD conjugated with agarose and then tested by immunoblotting with anti-Rac1 monoclonal antibody. Values were normalized against total Rac1. Graphs show data from four independent experiments; $*P<0.05$, $**P<0.01$. (C,D) Hippocampal neurons stimulated 4 hours with 10 μM fibrilar $A\beta_{1\text{-}42}$ were pre-treated with pertussis toxin and roscovitin. The GTP bound to Rac1 (C) and to Cdc42 (D) was determined using the Rac/Cdc42 Activation Assay Kit, according to manufacturer's recommendations. Values were normalized, with respect to total Rac1 and Cdc42; $*P<0.05$.

in the signaling pathway activated by Aβ that leads to increased actin polymerization, Rac1 and Cdc42 were inhibited by transiently expressing their dominant negative constructions. For this purpose, RacT17N-GFP and Cdc42T17N-GFP were transfected in neuronal cells stimulated with Aβ and in unstimulated cells. Transfections done with RacT17N-GFP or Cdc42T17N-GFP were able to inhibit increased F-actin (stained with Rhodamine-phalloidin) for untreated (data not shown) as well as for $A\beta_{1\text{-}42}$-stimulated cells (Fig. 6A, arrow), compared with neighboring untransfected cells (Fig. 6A, arrowheads). This effect was not obtained by transfecting GFP alone or constructs expressing wild-type or constitutive active forms of Rac1 and Cdc42 (data not shown). The F-actin decrease was then estimated by analyzing the fluorescence of Rhodamine-phalloidin staining. A decrease in F-actin of about 10% was obtained for control hippocampal neurons transfected with Rac1- and Cdc42-T17N forms, with respect to untransfected cells (Fig. 6B). For Aβ-treated hippocampal cells the difference between transfected and untransfected neurons was over 50% after the expression of the dominant negative forms of Rac1 and Cdc42 (Fig. 6B). These results demonstrate that Rac1 and Cdc42 are participating in the increase of actin polymerization mediated by $A\beta_{1\text{-}42}$.

Aβ mediates Rac1 activation through a mechanism dependent on Tiam1

Tiam1 requires translocation to the plasma membrane to induce cytoskeletal changes mediated by Rac1 (Michiels et al., 1997). To investigate whether Tiam1 is involved in Aβ-induced Rac1 stimulation, we examined the recruitment of Tiam1 from cytosolic to plasma membrane fraction. As shown in Fig. 7A, the membrane fraction is enriched 1.5-fold in Tiam1 after $A\beta_{1\text{-}42}$ treatment; this was time-dependent and there was a significant difference with controls, 4 hours after exposure to $A\beta_{1\text{-}42}$. This was the same time point at which Rac1 activation was found to be significantly increased (Fig. 3B). Phosphorylation of Thr residues of Tiam1 is another event that may elicit the activation and/or membrane translocation of the protein. In order to investigate the Tiam1 activation state we analyzed Tiam1 phosphorylation on Thr residue by using an antibody that recognizes phospho-Thr epitopes on total immunoprecipitated Tiam1. Fibrillar $A\beta_{1\text{-}42}$ induced a significant increase (1.5-fold) in the amount of Thr phosphorylation of Tiam1 (Fig. 7B).

Ca^{2+} signaling controls Tiam1 activation (Fleming et al., 1998), and also regulates translocation and activation of Rac (Price et al., 2003). We explored whether Aβ-induced Tiam1

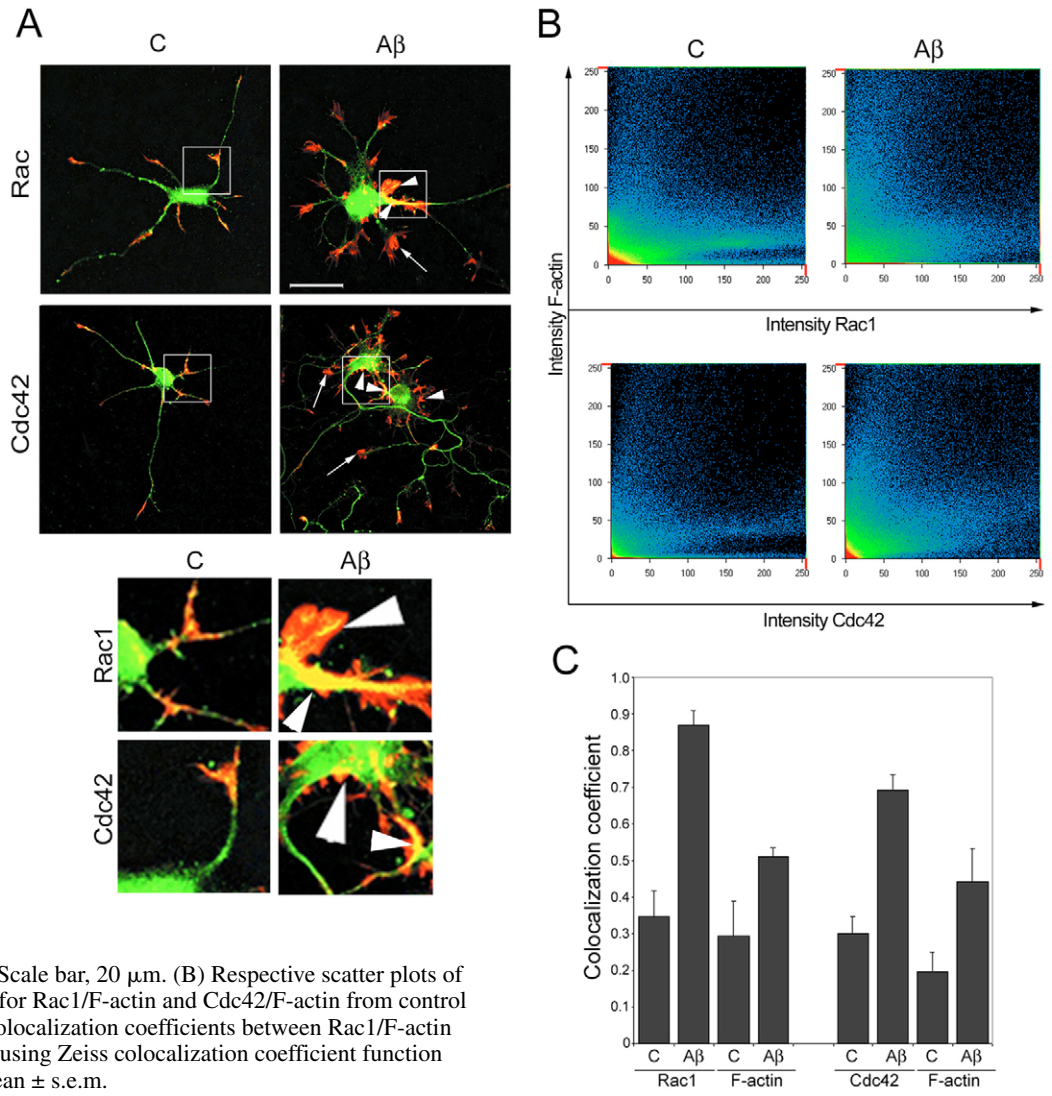

Fig. 4. Rac1 and Cdc42 display enhanced F-actin colocalization in hippocampal cells treated with Aβ. (A) Four-day hippocampal neurons, untreated (control) and exposed to $A\beta_{1\text{-}42}$ fibrils for 4 hours were double immunostained with Rac1 or Cdc42 and Rhodamine-phalloidin and analyzed by confocal laser-scanning microscopy. Images in the upper panel are overlays of Rac1 or Cdc42 vs. Rhodamine-phalloidin staining. Arrows indicate increased actin protusions in amyloid-stimulated neurons. Lower panels are higher magnification of the boxed regions showing Rac1 and Cdc42 overlaying with F-actin in control conditions, as well as the augmented colocalization of these proteins with F-actin (arrowhead) after Aβ stimulation. Scale bar, 20 μm. (B) Respective scatter plots of fluorescence intensity distribution for Rac1/F-actin and Cdc42/F-actin from control and Aβ-stimulated neurons. (C) Colocalization coefficients between Rac1/F-actin and Cdc42/F-actin were evaluated using Zeiss colocalization coefficient function software. Data are expressed as mean ± s.e.m.

and Rac1 activation is dependent on increases in intracellular Ca^{2+}. Fig. 8A shows a rapid enhancement of intracellular Ca^{2+} in neurons exposed to fibrillar $A\beta_{1\text{-}42}$. Such enhancement was sensitive to the addition of BAPTA-AM, which blocked this rise. In order to test whether Ca^{2+} affects Tiam1 activation by $A\beta_{1\text{-}42}$, Tiam1-threonine phosphorylation was examined by combining the addition of the fibrillar peptide with BAPTA-AM. Treatments with the Ca^{2+}chelator returned Tiam1-phosphothreonine expression to control levels (Fig. 8B). To confirm the Ca^{2+} involvement in Aβ-mediated Tiam1 activation, we analyzed whether BAPTA was affecting the amount of Tiam1 recovered after Rac1 was pulled down in a GTP-active form. Aβ treatments induce a higher association of Tiam1 with active Rac1. This increased co-immunoprecipitation was significantly reduced by combining BAPTA with Aβ treatments (Fig. 8C). PKC also seems to play a key role in Tiam1 activation (Fleming et al., 1997; Buchanan et al., 2000). Aβ treatments combined with the addition of Gö6976, a PKC inhibitor, also diminished Tiam1 co-immunoprecipitation with active Rac1 (Fig. 8C).

Calcium-dependent Rac activation involves the participation of a conventional PKC (Price et al., 2003). With the purpose of evaluating Ca^{2+} and PKC involvement in Aβ-mediated Rac1 activation, Rac1-GTP levels were examined in hippocampal cells stimulated with $A\beta_{1\text{-}42}$, along with BAPTA or Gö6976. The increase of Rac1 activation after $A\beta_{1\text{-}42}$ stimuli was inhibited when neurons were incubated with the peptide in the presence of BAPTA-AM (Fig. 9A). Inhibition of PKC also blocked the activation of Rac1 mediated by $A\beta_{1\text{-}42}$ (Fig. 9B).

Discussion

Stress stimuli such as $A\beta_{1\text{-}42}$, the main component of the amyloid plaque in AD, may alter the neuronal cytoskeleton. Here, we demonstrated that fibrillar $A\beta_{1\text{-}42}$ causes alterations in cytoskeletal actin in hippocampal cells, represented by an increase in the F-actin content. Alzheimer pathology is characterized by dramatic synapse and dendritic spine loss, as well as by damage in the synaptic terminal (Lippa et al., 1992; Masliah, 1995), where decreased cortical synapse density correlates with cognitive decline in patients (Terry et al., 1991; DeKosky et al., 1996). Aβ has been described to affect and accumulate in synapses (Takahashi et al., 2004). Likewise, a study using in vivo electrophysiology in the Tg2576 mouse model of AD showed disrupted cortical synaptic integration,

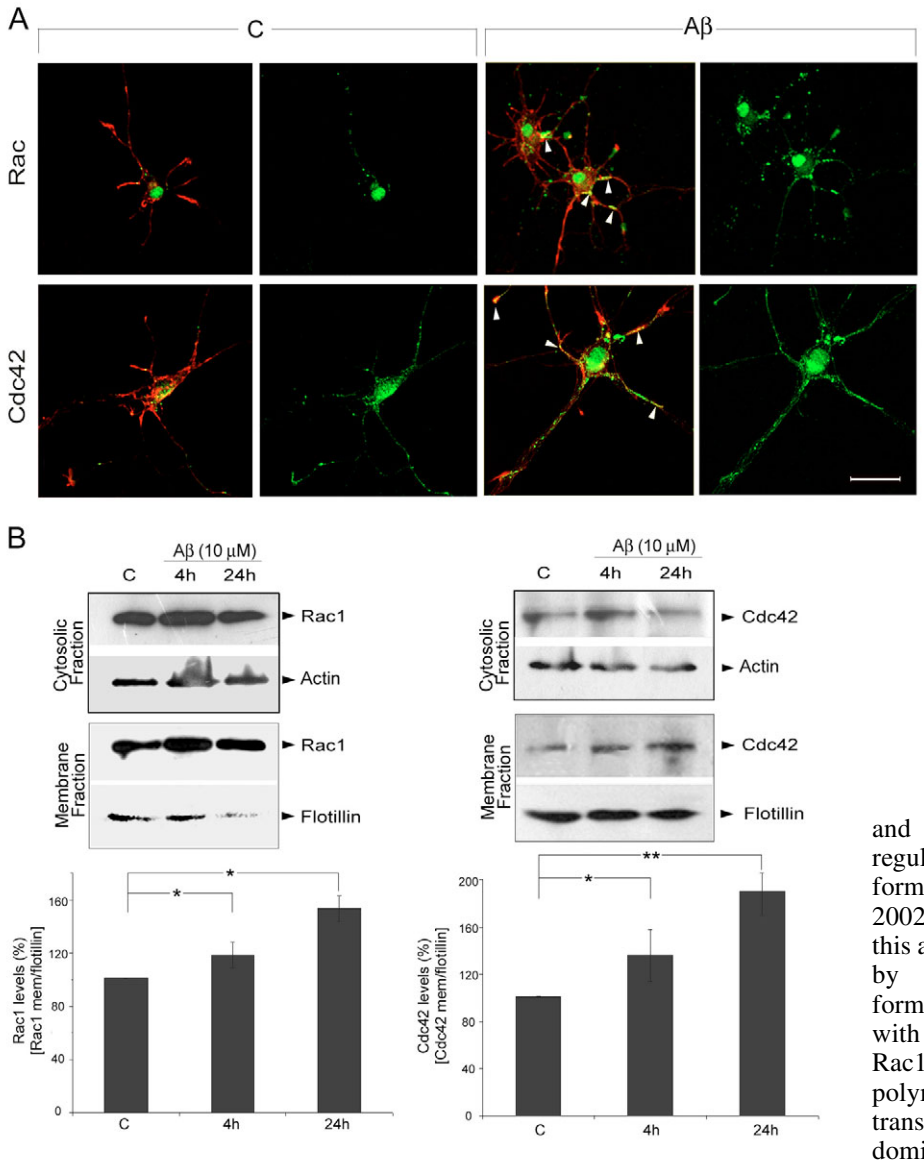

Fig. 5. Rac1 and Cdc42 increased in the plasma membrane after $A\beta_{1-42}$ stimulation. (A) Four-day hippocampal neurons, untreated (control) and exposed to $A\beta_{1-42}$ fibrils for 4 hours, were fixed after detergent extraction performed under cytoskeleton-stabilizing conditions and double immunostained with Rac1 or Cdc42 and Rhodamine-phalloidin. Both GTPases were recruited to the plasma membrane and were frequently found to colocalize with F-actin after amyloid stimulation (arrowheads). Bar, 20 μm. (B) Embryonic hippocampal cells, untreated and treated for 4 and 24 hours with β-amyloid, were lysed and cytoplasmic and membrane fractions obtained. Rho GTPases recruitment to the membrane fraction was analyzed using Rac1 and Cdc42 antibodies and the values were normalized against flotillin as a membrane protein control. Samples from the cytoplasmic fraction were analyzed by immunoblotting using Rac1 and Cdc42, along with actin antibody as a loading control. Significant differences are indicated by asterisks (*P<0.05, **P<0.01; Student's t-test).

which correlated with plaque formation (Stern et al., 2004). In a recent report using the Tg2576 transgenic mouse model, the same group described that spine loss is most pronounced near amyloid plaques, indicative of focal toxicity (Spires et al., 2005).

In this respect, the dynamic control of actin polymerization is considered critical for synaptic regulation and spine structure control (Matus, 2000; Halpain, 2000). Imbalance in actin dynamics has also been established to contribute to the formation of actin rods, leading to neurodegeneration (Minamide et al., 2000). Rod induction occurring in neurons exposed to stress accompanies damages mimicking neurodegenerative conditions. Alzheimer brain sections display rod-like inclusions, especially in areas surrounding the amyloid plaque, reinforcing the idea that Aβ peptide may play a role in the imbalance of actin dynamics (Maloney et al., 2005).

The dynamic actin-rich nature of dendritic spines has pointed to the Rho-GTPase family as a central contributor (Matus, 2000; Hering and Sheng, 2001; Etienne-Manneville and Hall, 2002), with Cdc42 and Rac1 regulating spine morphogenesis and synapse formation in neurons (Irie and Yamaguchi, 2002; Zhang et al., 2003). Here, we find that this augmented actin polymerization, as shown by increased lamellipodia and filopodia formation after $A\beta_{1-42}$ stimulus, is correlated with time- and dose-dependent increases in Rac1 and Cdc42 activity. The increased actin polymerization was inhibited in cells transfected with either Rac1 or Cdc42 dominant-negative forms, confirming the participation of these GTPases in the cascade of cellular events underlying the enhancement of F-actin by $A\beta_{1-42}$. Rac1 and Cdc42 have also been seen upregulated in neuronal populations of AD brains in comparison to controls (Zhu et al., 2000), and simultaneously overlapped with early cytoskeletal abnormalities, suggesting a physiological connection between these two processes in the context of AD. By contrast, a previous report demonstrated that Rac activation inhibits the formation of both dendritic spines and synapses (Zhang et al., 2003). In this sense, alterations of the synaptic efficacy along with a progressive loss in the number of dendritic spines, as have been described for AD pathology, could be a consequence of Rac1/Cdc42 activity deregulation.

One of the mechanisms that may be acting to increase Rac1 GTPase activity, as shown in this study, is the activation of Tiam1. Tiam1 was upregulated in both cortex and hippocampal cells stimulated with $A\beta_{1-42}$, reflected by increased threonine phosphorylation and enhanced membrane localization. The association of Tiam1 to the membrane accompanies its own activation and regulates different Rac-mediated signaling pathways, such as the induction of membrane ruffling through

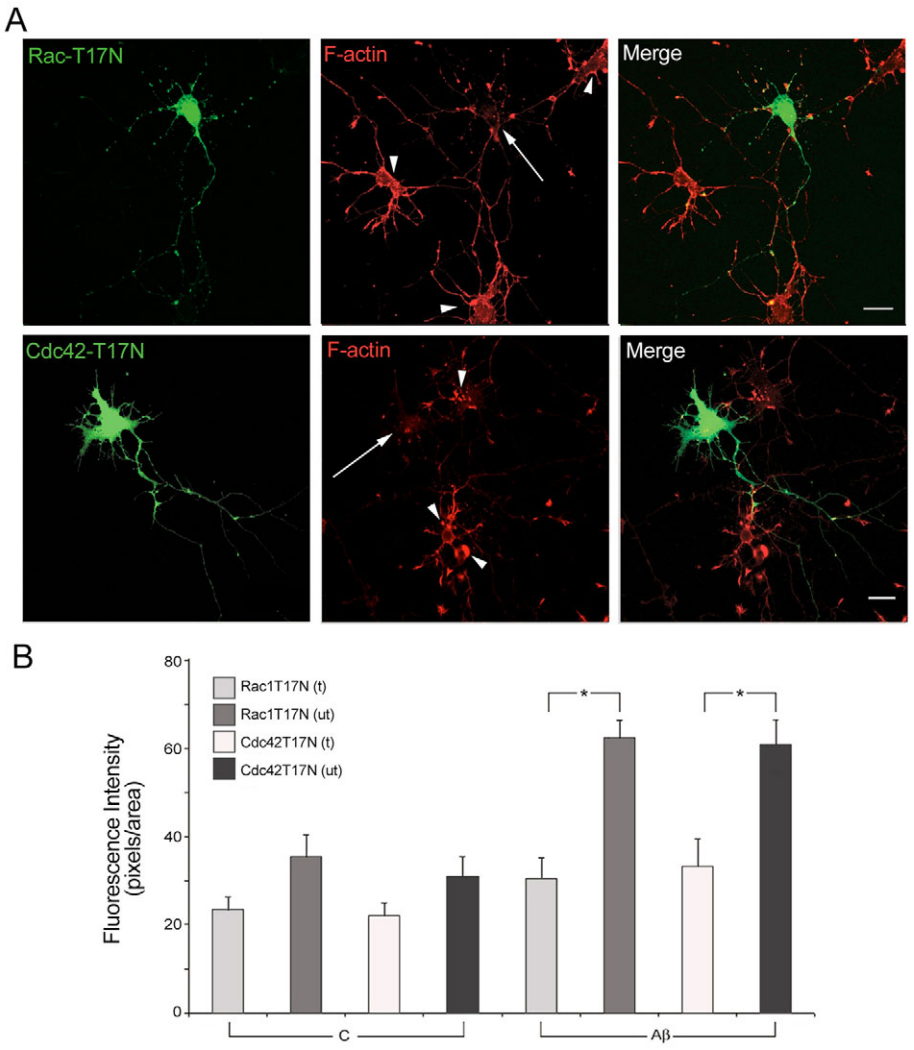

Fig. 6. Rac1 and Cdc42 are essential for the increased F-actin polymerization induced by $A\beta_{1\text{-}42}$ treatment. Primary hippocampal cells treated with $A\beta_{1\text{-}42}$ were transfected with the dominant negative forms of RacT17N-GFP and Cdc42T17N-GFP (arrows), and then stained for F-actin using Rhodamine-phalloidin. The untransfected neurons are indicated by arrowheads. Scale bar, 20 μm. (B) Changes in F-actin levels were determined and differences between transfected (t) vs. untransfected (ut) control and Aβ-stimulated neurons were determined using Student's *t*-test. The values were expressed as mean ± s.e.m. for three different experiments, with at least 12 determinations per experiment; **P*<0.05.

Rac1 (Michiels et al., 1997). In this sense, we detected that treatment with $A\beta_{1\text{-}42}$ induced membrane ruffle formation in hippocampal cells, implying that Tiam1 participates in Aβ-mediated Rac1 upregulation. In addition, an increase in Tiam1 association with the active form of Rac1 (Rac-GTP) after stimulus with $A\beta_{1\text{-}42}$ was established, confirming the direct involvement of this GEF in Rac1 activation in the amyloigenic context. However, our experiments do not exclude the existence of other regulators, and additional mechanisms may also be playing a role.

Changes in Ca^{2+} homeostasis, as occurring after Aβ addition, may influence several physiological responses contributing to neuronal imbalance. Here, we demonstrate that Ca^{2+} is involved in the enhanced Tiam1 and Rac1 activity induced by Aβ. PKC may also be acting, since PKC inhibition affects Tiam1 association with the active form of Rac-coupling GTP, as well as Rac1 activity in hippocampal neurons stimulated with $A\beta_{1\text{-}42}$. Altogether these results illustrate that Tiam1 upregulation is responsible for increased Rac1 activity in the hippocampus, by stimulus with fibrillar Aβ.

Recent studies report more robust correlations between the levels of soluble, rather than insoluble, Aβ and the extent of synaptic loss and severity of cognitive impairment (Lue et al., 1999; McLean et al., 1999; Wang et al., 1999).

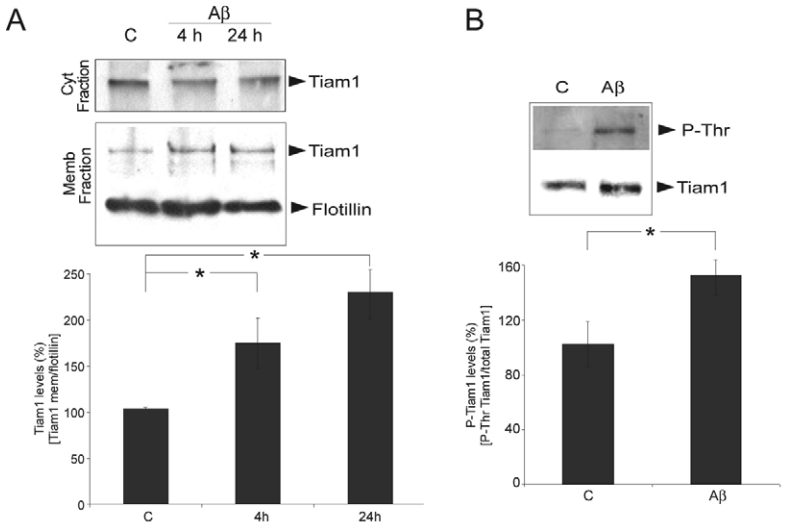

Fig. 7. Tiam1 is activated in Aβ-stimulated hippocampal cells. (A) Membrane fractions from hippocampal cells, either untreated (control) and stimulated for 4 and 24 hours with 10 μM of fibrillar $A\beta_{1\text{-}42}$, were obtained. Samples were analyzed by immunoblotting using Tiam1 antibody and the values were normalized against flotillin. Tiam1 expression in the cytoplasmic fraction was analyzed by immunoblotting using Tiam1 antibody and actin as a loading control. (B) Tiam1 was immunoprecipitated from control hippocampal neurons and neurons treated for 4 hours with $A\beta_{1\text{-}42}$. Phosphorylation levels were tested by immunoblotting using P-Thr monoclonal antibody. **P*<0.05.

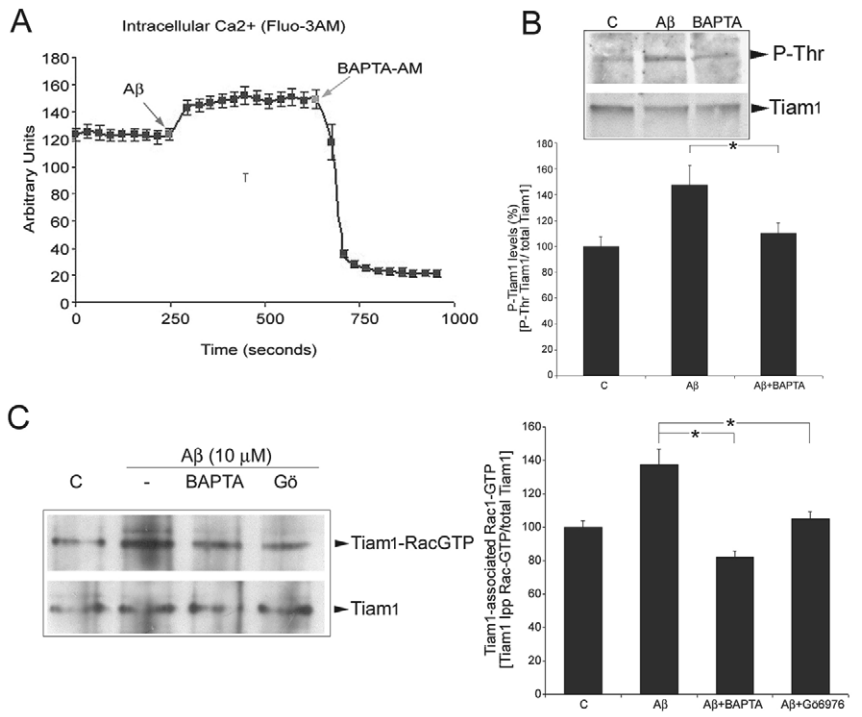

Fig. 8. Aβ-mediated Tiam1 activation is affected by Ca^{2+} signaling. (A) Time lapse experiments were performed to analyze the Ca^{2+} increase in hippocampal cells after $A\beta_{1-42}$ addition, using the fluorescent tracer Fluo3-AM. (B) Phospho-Thr levels from total immunoprecipitated Tiam1 were tested by immunoblot, in neurons treated with $A\beta_{1-42}$ in the presence of BAPTA-AM; $^*P<0.05$. (C) Hippocampal neurons stimulated with $A\beta_{1-42}$ were analyzed for Tiam1 association to active Rac1 after BAPTA-AM or Gö6976 treatments. Rac1 was pulled down using PAK-PBD agarose and the co-immunoprecipitated Tiam1 was tested by immunoblotting using anti-Tiam1 antibody. Values were normalized against total Tiam1 in the crude homogenized. $^*P<0.05$.

Therefore, the increased actin polymerization observed after fibrillar Aβ stimulation could be generated to counteract the synaptic damage by the soluble form of the amyloid peptide, rescuing neurons from the loss of synaptic plasticity. Nevertheless, a continued increase of actin dynamics, as a consequence of Rho GTPases deregulation by Aβ stimulation, could end in an exacerbated accumulation of F-actin. This event would be the trigger for the formation of F-actin aggregates, as those described in Hirano bodies in Alzheimer pathology (Gibson and Tomlinson, 1977).

Our findings demonstrate a direct relationship of Aβ with Rac1/Cdc42 Rho GTPases deregulation and subsequent actin cytoskeletal alterations. These results are of interest because one of the deleterious effects in the pathway to Alzheimer's disease could be related to alterations in the normal actin turnover. In summary, these results points to the actin cytoskeleton as a target for Aβ-induced neurodegeneration in Alzheimer's disease.

Materials and Methods

Reagents

Rhodamine-phalloidin, pertussis toxin, protein A-agarose, monoclonal antibodies anti-actin and Tub-Tyr were from Sigma (Sigma-Aldrich). Polyclonal antibodies for Cdc42 (P1), NFkB (H119), LIMK1 (C18) and Tiam1 (C16) were purchased from Santa Cruz Biotechnology Inc. (Santa Cruz, CA, USA). Polyclonal anti-P-LIMK was from Cell Signaling (Cell Signaling Technology, Beverly, MA). Monoclonal flotillin 1 antibody was purchased from BD Transduction Laboratories (BD Biosciences). Beta amyloid$_{1-42}$ peptide was from Global Peptide Services, CO. The Rac/Cdc42 activation assay kit and monoclonal anti-Rac1 antibody were purchased from Upstate Biotechnology Inc. (Lake Placid, NY). Phospho-Thr antibody was from Biodesign International. The following secondary antibodies were used: anti-mouse (Jackson ImmunoResearch), and anti-rabbit (Pierce Biotechnology), both horseradish peroxidase conjugated; anti-rabbit FITC-coupled (Sigma-Aldrich) and antimouse FITC-coupled (Jackson ImmunoResearch). BAPTA-AM, Gö6976 and roscovitine were purchased from Calbiochem. The Western Lighting Chemiluminescence Reagent Plus was from Perkin Elmer. The Actin Polymerization Assay Biochem Kit was from Cytoskeleton (Denver, CO). Neurobasal (NB), B27, Opti-MEM and Lipofectamine-2000 were from Invitrogen-Gibco-BRL Life Technologies. All other chemicals were obtained from usual commercial sources at the highest grade available.

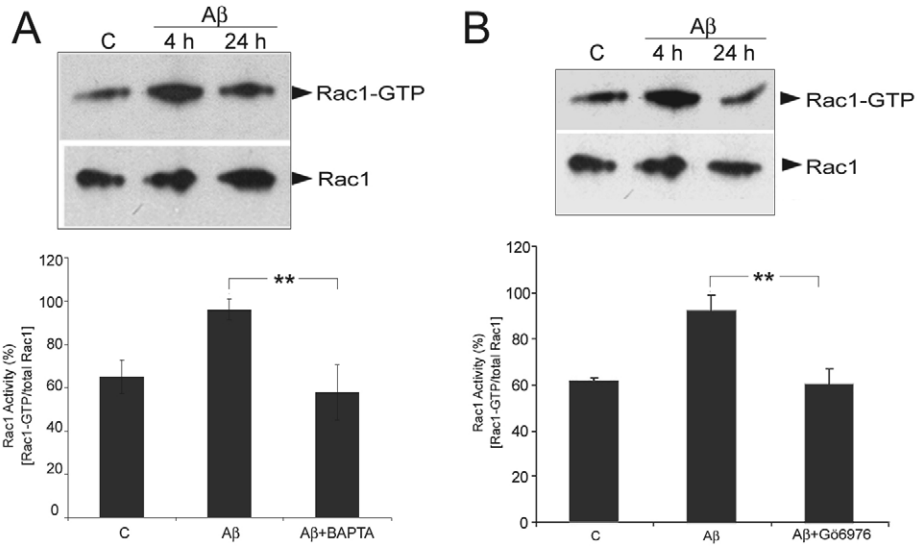

Fig. 9. Tiam1 mediates Rac1 activation through Ca^{2+} signaling in Aβ-stimulated hippocampal cells. Hippocampal neurons were incubated for 4 hours with $A\beta_{1-42}$ in the presence of BAPTA-AM (A) or Gö6976 (B) and then the active Rac1 fraction was pulled-down using the PAK-PBD binding domain. The active form of Rac1 was revealed using Rac1 monoclonal antibody. $^{**}P<0.01$.

Cell cultures

Dissociated hippocampal and cortex cultures were prepared from E19 embryos of Sprague-Dawley rats as described previously (Caceres et al., 1986). Cells were plated onto poly-D-lysine-coated plates and coverslips and maintained with NB plus 10% horse serum. Three hours after plating the medium was removed and serum-free medium B27/NB was added. Hippocampal and cortical neurons were maintained for 4 days before treatments.

Preparation of Aβ aggregated peptide

$A\beta_{1-42}$ peptide was prepared by dissolving the lyophilized synthetic peptide in DMSO (6.67%) and phosphate buffer at pH 7.4, diluted to a concentration of 1 μg/μl and aggregated according to the 'Aged condition' protocol (Pike et al., 1993) with some modifications (25°C for 7 days under vigorous agitation). Fibrillar $A\beta_{1-42}$ was characterized by negative staining with uranyl acetate and morphologically analyzed by electron microscopy [JEOL 100SX (100 kV)].

Immunofluorescence

Hippocampal neurons exposed to $A\beta_{1-42}$ fibrils for 4 hours were: (1) fixed with 4% paraformaldehyde plus 4% sucrose in phosphate buffer, pH 7.2 for 10 minutes and permeabilized with 0.1% Triton X-100; or (2) extracted with detergent to prepare 'cytoskeleton fractions' according to the procedure of Brown (Brown et al., 1992), then washed for 30 seconds with PHEM buffer pH 6.9 (60 mM Pipes, 25 mM HEPES, 10 mM EGTA, 2 mM $MgCl_2$) followed by extraction (2 minutes) with 0.2% saponin in PHEM buffer containing 10 mM taxol. The cells were then fixed for 20 minutes with warmed 2% paraformaldehyde-0.05% glutaraldehyde in PHEM buffer. The cells were incubated with the respective antibodies in 2.5% BSA-PBS in a humid chamber at 4°C overnight. Rhodamine-phalloidin was included for visualization of F-actin. The cells were examined by confocal laser scanning microscopy (LSM 510; Carl Zeiss MicroImaging, Inc.).

F-actin quantification

The concentration of F-actin in control untreated and 4 and 24 hours Aβ-treated hippocampal cells was measured with an Actin Polymerization Assay Kit, according to the manufacturer's recommendations. The cells were homogenized in F-actin stabilization buffer, pH 6.9 plus protease and phosphatase inhibitors. Phalloidin at 1 μM was used as a positive control. Equal amounts of protein were: (a) analyzed by western blotting using actin polyclonal antibody, and (b) centrifuged, first at 600 ***g*** to separate the nuclear fraction and then at 100,000 ***g*** for 60 minutes at 30°C. The pellets, corresponding to the F-actin fractions, were re-suspended in ice-cold H_2O plus 1 μM cytochalasin D. They were then incubated on ice for 1 hour to dissociate F-actin. The resuspended pellets were gently mixed every 15 minutes. SDS sample buffer was added and the fractions were separated by 10% SDS-PAGE, electroblotted onto nitrocellulose sheets and visualized with anti-actin antibody, with Western Lighting Chemiluminescence Reagent Plus (Perkin Elmer). The ratio of F-actin/total actin bands was determined by scanning and quantifying densitometry in a Kodak Digital Science 1D 3.0.2 densitometer.

Image analysis

For the semi-quantitative measurement of the F-actin content, control and treated hippocampal neurons were immunostained with phalloidin-Rhodamin. All pictures were analyzed with the Carl Zeiss LSM 510 Image Browser program. Fluorescence intensity was calculated by averaging the fluorescence intensity of all pixels and subtracting the non-specific background from outside the cell. Each value is the mean (± s.e.m.) of three different experiments, with at least 12 determinations in each experiment. Differences were evaluated with the Student's *t*-test. Colocalization coefficients were calculated using Zeiss colocalization coefficient function software, where all pixels above background are taken into account and the relative number of colocalizing pixels in channels (Ch2: green and Ch3: red) are calculated compared to total number of pixels above threshold. For a particular color (e.g. red), the colocalization coefficient represents the ratio of red pixel intensities showing a green component divided by the sum of all red intensities. Data are presented as a value between 0 and 1, where 0 indicates no colocalization and 1 indicates that all pixels colocalize (Smallcombe, 2001), and are expressed as mean ± s.e.m. Colocalization analysis data were obtained from more than 16 double-labeled cells in three different experiments.

Morphometric analysis

Morphometric parameters were evaluated in cells stained with Rhodamine-conjugated phalloidin. The number of filopodia and the area of the growth cone (expressed in μm^2) of hippocampal neurons stimulated with 10 μM $A\beta_{1-42}$ for 4 hours were analyzed, using a Zeiss LSM 510 confocal microscope with the Carl Zeiss LSM Image Examiner program. The growth cone was defined as the distal part of the neurite where the diameter is twice that of the neurite itself (Bradke and Dotti, 1997). Filopodial number was determined per growth cone. Processes and growth cones were randomly selected.

Rac1 and Cdc42 activation assay

Hippocampal neurons were treated with 0.1, 1 and 10 μM of fibrillar $A\beta_{1-42}$ for 24 hours as well as with 10 μM $A\beta_{1-42}$ for 30 minutes, 2, 4 and 24 hours. The GTP loading of Rac1 and Cdc42 was measured using a Rac1/Cdc42 Activation Assay Kit, according to manufacturer's recommendations. Values of Rac/Cdc42 activation were expressed as the ratio of Rac1-GTP or Cdc42-GTP/total Rac1 or Cdc42 in the crude extract. For some experiments, cells were treated with 10 μg/ml of roscovitin inhibitor or pre-treated 4 hours with pertussis toxin at 500 ng/ml, plus 24 hours stimulation with 10 μM $A\beta_{1-42}$. Hippocampal neurons were also stimulated for 4 hours with 10 μM $A\beta_{1-42}$ in the presence or absence of 15 μM BAPTA-AM or 1 μM Gö6976, both incubated for 1 hour (BAPTA-AM and Gö6976 were added 3 hours after Aβ stimulus). Tiam1 pulled down with active Rac1 was evaluated using anti-Tiam1 antibody. The ratio of Tiam1 pulled down with Rac-GTP/total Tiam1 in the crude protein extract was determined by scanning and quantifying densitometry in a Kodak Digital Science 1D 3.0.2 densitometer.

Subcellular fractionation experiments

Hippocampal neurons untreated or stimulated for 4 and 24 hours with 10 μM Aβ, as well as 4 hours with 10 μM Aβ in the presence of 15 μM BAPTA-AM incubated 1 hour, were lysed in STM buffer and the membrane fractions were obtained according to the protocol of Nikolic et al. (Nikolic et al., 1998). Pellets and supernatants were re-suspended in Laemmli 4× sample buffer and analyzed by immunoblotting using Rac1, Cdc42, Tiam1, flotillin, actin and NFκB antibodies and a Western Lighting Chemiluminescence Reagent Plus.

Immunoprecipitation

Protein extracts were prepared from control and 4 hours Aβ-treated hippocampal neurons in RIPA buffer plus protease and phosphatase inhibitors as we previously described (Alvarez et al., 2001). Tiam1 polyclonal antibody (4 μl) was incubated at 4°C overnight. The samples were separated by SDS-PAGE, electroblotted onto nitrocellulose sheets, and visualized with P-Thr and Tiam1 antibodies using Western Lighting Chemiluminescence Reagent Plus. Bands were quantified in a Kodak Digital Science 1D 3.0.2 densitometer.

DNA plasmids and transfection

Plasmids encoding dominant negative mutant (T17N) of the GTPases Rac1 and Cdc42 were sub-cloned in a plasmid encoding green fluorescence protein pEGFP-C1 (Clontech, Palo Alto, CA) by a *Hin*dIII and *Apa*I digestion. These vectors were transfected in primary hippocampal neurons, using Opti-MEM buffer and Lipofectamine 2000, according to the manufacturer's recommendations. After 4 hours the medium was replaced by NB/B27 and the cells were maintained in culture for a further 24 hours. The neurons were then stimulated with 10 μM $A\beta_{1-42}$ for 4 hours. Transfected and non-transfected neurons were analyzed by immunofluorescence.

Measurement of Ca^{2+} transients

An LSM 510 laser-scanning confocal microscope was used for analysis of Ca^{2+} transients in hippocampal neurons loaded with Fluo3-AM [prepared by mixing of 2 μM dye solution in DMSO with Pluronic acid (20% in DMSO)]. The Fluo3-AM dye was incubated for 30 minutes at 37°C and 5% CO_2 at a final concentration of 5 μM in Krebs-Ringer/HEPES buffer pH 7.4 (KRH; 115 mM NaCl, 5 mM KCl, 1 mM potassium phosphate, 5 mM glucose, 1.5 mM $CaCl_2$, 1.2 mM $MgSO_4$, 25 mM HEPES pH 7.4). After the dye was removed, the cells were washed twice with fresh KRH buffer. Using a time-lapse series of images, Ca^{2+} transients were analyzed before, during, and after stimulation of the neurons with 10 μM $A\beta_{1-42}$ fibrils and with 15 μM of BAPTA-AM Ca^{2+} chelator.

Statistics

Results were analyzed using with Student's *t*-test. Results were expressed as mean ± s.d., or mean ± s.e.m. $P<0.05$ was considered to be significant.

This work was supported by grants from FONDECYT 1050198 to R.B.M. and by the Millennium Institute CBB. A.M.-N. was supported by a doctoral fellowship from the Millennium Institute for Advanced Studies in Cell Biology and Biotechnology (CBB). We are grateful to Alexandra Ginesta for critically reading the manuscript.

References

Alvarez, A., Toro, R., Caceres, A. and Maccioni, R. B. (1999). Inhibition of tau phosphorylating protein kinase cdk5 prevents beta-amyloid-induced neuronal death. *FEBS Lett.* **459**, 421-426.

Alvarez, A., Munoz, J. P. and Maccioni, R. B. (2001). A Cdk5-p35 stable complex is involved in the beta-amyloid-induced deregulation of Cdk5 activity in hippocampal neurons. *Exp. Cell Res.* **264**, 266-274.

Bishop, A. L. and Hall, A. (2000). Rho GTPases and their effector proteins. *Biochem. J.* **348**, 241-255.

Bradke, F. and Dotti, C. G. (1997). Neuronal polarity: vectorial cytoplasmic flow precedes axon formation. *Neuron* **19**, 1175-1186.

Brown, A., Slaughter, T. and Black, M. M. (1992). Newly assembled microtubules are

concentrated in the proximal and distal regions of growing axons. *J. Cell Biol.* **119**, 867-882.

Buchanan, F. G., Elliot, C. M., Gibbs, M. and Exton, J. H. (2000). Translocation of the Rac1 guanine nucleotide exchange factor Tiam1 induced by platelet-derived growth factor and lysophosphatidic acid. *J. Biol. Chem.* **275**, 9742-9748.

Caceres, A., Banker, G. A. and Binder, L. (1986). Immunocytochemical localization of tubulin and microtubule-associated protein 2 during the development of hippocampal neurons in culture. *J. Neurosci.* **6**, 714-722.

DeKosky, S. T., Scheff, S. W. and Styren, S. D. (1996). Structural correlates of cognition in dementia: quantification and assessment of synapse change. *Neurodegeneration* **5**, 417-421.

Etienne-Manneville, S. and Hall, A. (2002). Rho GTPases in cell biology. *Nature* **420**, 629-635.

Fleming, I. N., Elliott, C. M., Collard, J. G. and Exton, J. H. (1997). Lysophosphatidic acid induces threonine phosphorylation of Tiam1 in Swiss 3T3 fibroblasts via activation of protein kinase C. *J. Biol. Chem.* **272**, 33105-33110.

Fleming, I. N., Elliott, C. M. and Exton, J. H. (1998). Phospholipase C-gamma, protein kinase C and Ca2+/calmodulin-dependent protein kinase II are involved in platelet-derived growth factor-induced phosphorylation of Tiam1. *FEBS Lett.* **429**, 229-233.

Fleming, I. N., Elliott, C. M., Buchanan, F. G., Downes, C. P. and Exton, J. H. (1999). Ca2+/calmodulin-dependent protein kinase II regulates Tiam1 by reversible protein phosphorylation. *J. Biol. Chem.* **274**, 12753-12758.

Funato, H., Yoshimura, M., Kusui, K., Tamaoka, A., Ishikawa, K., Ohkoshi, N., Namekata, K., Okeda, R. and Ihara, Y. (1998). Quantitation of amyloid beta-protein (A beta) in the cortex during aging and in Alzheimer's disease. *Am. J. Pathol*. **152**, 1633-1640.

Galloway, P. G., Perry, G. and Gambetti, P. (1987). Hirano body filaments contain actin and actin-associated proteins. *J. Neuropathol. Exp. Neurol.* **46**, 185-199.

Gibson, P. H. and Tomlinson, B. E. (1977). Numbers of Hirano bodies in the hippocampus of normal and demented people with Alzheimer's disease. *J. Neurol. Sci.* **33**, 199-206.

Goldman, J. E. (1983). The association of actin with Hirano bodies. *J. Neuropathol. Exp. Neurol.* **42**, 146-152.

Habets, G. G., Scholtes, E. H., Zuydgeest, D., van der Kammen, R. A., Stam, J. C., Berns, A. and Collard, J. G. (1994). Identification of an invasion-inducing gene, Tiam-1, that encodes a protein with homology to GDP-GTP exchangers for Rho-like proteins. *Cell* **77**, 537-549.

Halpain, S. (2000). Actin and the agile spine: how and why do dendritic spines dance? *Trends Neurosci.* **23**, 141-146.

Hering, H. and Sheng, M. (2001). Dendritic spines: structure, dynamics and regulation. *Nat. Rev. Neurosci.* **2**, 880-888.

Hsiao, K., Chapman, P., Nilsen, S., Eckman, C., Harigaya, Y., Younkin, S., Yang, F. and Cole, G. (1996). Correlative memory deficits, Abeta elevation, and amyloid plaques in transgenic mice. *Science* **274**, 99-102.

Irie, F. and Yamaguchi, Y. (2002). EphB receptors regulate dendritic spine development via intersectin, Cdc42 and N-WASP. *Nat. Neurosci.* **5**, 1117-1118.

Kawarabayashi, T., Younkin, L. H., Saido, T. C., Shoji, M., Ashe, K. H. and Younkin, S. G. (2001). Age-dependent changes in brain, CSF, and plasma amyloid (beta) protein in the Tg2576 transgenic mouse model of Alzheimer's disease. *J. Neurosci*. **21**, 372-381.

Kozma, R., Ahmed, S., Best, A. and Lim, L. (1995). The Ras-related protein Cdc42Hs and bradykinin promote formation of peripheral actin microspikes and filopodia in Swiss 3T3 fibroblasts. *Mol. Cell. Biol.* **15**, 1942-1952.

Kuo, Y. M., Emmerling, M. R., Lampert, H. C., Hempelman, S. R., Kokjohn, T. A., Woods, A. S., Cotter, R. J. and Roher, A. E. (1999). High levels of circulating Abeta42 are sequestered by plasma proteins in Alzheimer's disease. *Biochem. Biophys. Res. Commun*. **257**, 787-791.

Lee, M., You, H. J., Cho, S. H., Woo, C. H., Yoo, M. H., Joe, E. H. and Kim, J. H. (2002). Implication of the small GTPase Rac1 in the generation of reactive oxygen species in response to beta-amyloid in C6 astroglioma cells. *Biochem. J.* **366**, 937-943.

Lippa, C. F., Hamos, J. E., Pulaski-Salo, D., DeGennaro, L. J. and Drachman, D. A. (1992). Alzheimer's disease and aging: effects on perforant pathway perikarya and synapses. *Neurobiol. Aging* **13**, 405-411.

Lue, L. F., Kuo, Y. M., Roher, A. E., Brachova, L., Shen, Y., Sue, L., Beach, T., Kurth, J. H., Rydel, R. E. and Rogers, J. (1999). Soluble amyloid beta peptide concentration as a predictor of synaptic change in Alzheimer's disease. *Am. J. Pathol.* **155**, 853-862.

Luo, L. (2000). Rho GTPases in neuronal morphogenesis. *Nat. Rev. Neurosci.* **1**, 173-180.

Maloney, M. T., Minamide, L. S., Kinley, A. W., Boyle, J. A. and Bamburg, J. R. (2005). Beta-secretase-cleaved amyloid precursor protein accumulates at actin inclusions induced in neurons by stress or amyloid beta: a feedforward mechanism for Alzheimer's disease. *J. Neurosci.* **25**, 11313-11321.

Masliah, E. (1995). Mechanisms of synaptic dysfunction in Alzheimer's disease. *Histol. Histopathol.* **10**, 509-519.

Mattson, M. P., Barger, S. W., Cheng, B., Lieberburg, I., Smith-Swintosky, V. L. and Rydel, R. E. (1993). beta-Amyloid precursor protein metabolites and loss of neuronal Ca2+ homeostasis in Alzheimer's disease. *Trends Neurosci.* **16**, 409-414.

Matus, A. (2000). Actin-based plasticity in dendritic spines. *Science* **290**, 754-758.

McLean, C. A., Cherny, R. A., Fraser, F. W., Fuller, S. J., Smith, M. J., Beyreuther, K., Bush, A. I. and Masters, C. L. (1999). Soluble pool of Abeta amyloid as a determinant of severity of neurodegeneration in Alzheimer's disease. *Ann. Neurol.* **46**, 860-866.

Michiels, F., Stam, J. C., Hordijk, P. L., van der Kammen, R. A., Ruuls-Van Stalle, L., Feltkamp, C. A. and Collard, J. G. (1997). Regulated membrane localization of Tiam1, mediated by the NH2-terminal pleckstrin homology domain, is required for Rac-dependent membrane ruffling and C-Jun NH2-terminal kinase activation. *J. Cell Biol.* **137**, 387-398.

Minamide, L. S., Striegl, A. M., Boyle, J. A., Meberg, P. J. and Bamburg, J. R. (2000). Neurodegenerative stimuli induce persistent ADF/cofilin-actin rods that disrupt distal neurite function. *Nat. Cell. Biol.* **2**, 628-636.

Nakayama, A. Y., Harms, M. B. and Luo, L. (2000). Small GTPases Rac and Rho in the maintenance of dendritic spines and branches in hippocampal pyramidal neurons. *J. Neurosci*. **20**, 5329-5338.

Nikolic, M., Chou, M. M., Lu, W., Mayer, B. J. and Tsai, L. H. (1998). The p35/Cdk5 kinase is a neuron-specific Rac effector that inhibits Pak1 activity. *Nature* **395**, 194-198.

Nobes, C. D. and Hall, A. (1995). Rho, rac, and cdc42 GTPases regulate the assembly of multimolecular focal complexes associated with actin stress fibers, lamellipodia, and filopodia. *Cell* **81**, 53-62.

Otth, C., Mendoza-Naranjo, A., Mujica, L., Zambrano, A., Concha, I. I. and Maccioni, R. B. (2003). Modulation of the JNK and p38 pathways by cdk5 protein kinase in a transgenic mouse model of Alzheimer's disease. *NeuroReport* **14**, 2403-2409.

Patrick, G. N., Zukerberg, L., Nikolic, M., de la Monte, S., Dikkes, P. and Tsai, L. H. (1999). Conversion of p35 to p25 deregulates Cdk5 activity and promotes neurodegeneration. *Nature* **402**, 615-622.

Pike, C. J., Burdick, D., Walencewicz, A. J., Glabe, C. G. and Cotman, C. W. (1993). Neurodegeneration induced by beta-amyloid peptides in vitro: the role of peptide assembly state. *J. Neurosci.* **13**, 1676-1687.

Price, L. S., Langeslag, M., ten Klooster, J. P., Hordijk, P. L., Jalink, K. and Collard, J. G. (2003). Calcium signaling regulates translocation and activation of Rac. *J. Biol. Chem.* **278**, 39413-39421.

Ridley, A. J., Paterson, H. F., Johnston, C. L., Diekmann, D. and Hall, A. (1992). The small GTP-binding protein rac regulates growth factor-induced membrane ruffling. *Cell* **70**, 401-410.

Schmitz, A. A., Govek, E. E., Bottner, B. and Van Aelst, L. (2000). Rho GTPases: signaling, migration, and invasion. *Exp. Cell Res.* **261**, 1-12.

Seabra, M. C. (1998). Membrane association and targeting of prenylated Ras-like GTPases. *Cell Signal.* **10**, 167-172.

Smallcombe, A. (2001). Multicolor imaging: the important question of co-localization. *Biotechniques* **30**, 1240-1242, 1244-1246.

Spires, T. L., Meyer-Luehmann, M., Stern, E. A., McLean, P. J., Skoch, J., Nguyen, P. T., Bacskai, B. J. and Hyman, B. T. (2005). Dendritic spine abnormalities in amyloid transgenic mice demonstrated by gene intravital multiphoton microscopy. *J. Neurosci.* **25**, 7278-7287.

Stern, E. A., Bacskai, B. J., Hickey, G. A., Attenello, F. J., Lombardo, J. A. and Hyman, B. T. (2004). Cortical synaptic integration *in vivo* is disrupted by amyloid-plaques. *J. Neurosci.* **24**, 4535-4540.

Takahashi, R. H., Almeida, C. G., Kearney, P. F., Yu, F., Lin, M. T., Milner, T. A. and Gouras, G. K. (2004). Oligomerization of Alzheimer's beta-amyloid within processes and synapses of cultured neurons and brain. *J. Neurosci.* **24**, 3592-3599.

Terry, R. D., Masliah, E., Salmon, D. P., Butters, N., DeTeresa, R., Hill, R., Hansen, L. A. and Katzman, R. (1991). Physical basis of cognitive alterations in Alzheimer's disease: synapse loss is the major correlate of cognitive impairment. *Ann. Neurol.* **30**, 572-580.

Van Leeuwen, F. N., Olivo, C., Grivell, S., Giepmans, B. N., Collard, J. G. and Moolenaar, W. H. (2003). Rac activation by lysophosphatidic acid LPA1 receptors through the guanine nucleotide exchange factor Tiam1. *J. Biol. Chem.* **278**, 400-406.

Wang, J., Dickson, D. W., Trojanowski, J. Q. and Lee, V. M. (1999). The levels of soluble versus insoluble brain Abeta distinguish Alzheimer's disease from normal and pathologic aging. *Exp. Neurol.* **158**, 328-337.

Zhang, H., Webb, D. J., Asmussen, H. and Horwitz, A. F. (2003). Synapse formation is regulated by the signaling adaptor GIT1. *J. Cell Biol.* **161**, 131-142.

Zhu, X., Raina, A. K., Boux, H., Simmons, Z. L., Takeda, A. and Smith, M. A. (2000). Activation of oncogenic pathways in degenerating neurons in Alzheimer disease. *Int. J. Dev. Neurosci.* **18**, 433-437.